SIMULATION OF SEMICONDUCTOR DEVICES AND PROCESSES Vol. 5
Edited by S. Selberherr, H. Stippel, E. Strasser – September 1993

A Powerful TCAD System Including Advanced RSM Techniques for Various Engineering Optimization Problems

R. Cartuyvels, R. Booth[†], S. Kubicek, L. Dupas, and K. M. De Meyer

IMEC
Kapeldreef 75, B-3001 Leuven, BELGIUM
[†]AT&T
1247 South Cedar Crest Blvd., Allentown, PA 18103, USA

Abstract

This paper presents the NORMAN/DEBORA TCAD system developed at IMEC to design and optimize sub-micron IC technology using process and device simulators. The versatility of the TCAD system will be shown for two important problems encountered in IC technology design and optimization.

1. Introduction

TCAD systems have become indispensable tools to investigate various engineering problems in the field of IC technology. Process design and optimization problems, simulator calibration and sensitivity analysis across several design levels (process → device → circuit) can be handled with an increasing efficiency using the automated coupling features a TCAD system provides. Although simulation provides a cheap way to experiment, it still remains quite CPU-time intensive, even if the TCAD system creates a fully automated environment. We have adopted the concepts of the Response Surface Methodology (RSM), which have been successfully used in various experimental fields [1], to efficiently plan a number of simulation experiments using the TCAD system to schedule and sequence them automatically. For these purposes, we developed an open TCAD system (NORMAN) including a novel design of experiments concept (Target Oriented Design), a unique parameter transformation technique to improve the fitting accuracy of the response models and a non-linearly constrained optimizer (DEBORA). We'll discuss its use in a few of the previously mentioned engineering problems.

2. Process design and optimization

Designing a process involves determining the settings of a high number of control variables such that a number of constraints upon device or circuit characteristics are met (figure 1). Optimizing the process is improving the process design such that an objective is optimized. Several objectives can be defined : minimize the process sensitivity w.r.t. to disturbances upon variables (e.g. an implantation dose), minimize the characteristic's target deviations, ...The mathematical formulation for minimizing the process sensitivity is shown in figure 2. $R_j(\vec{x})$ denotes response j (e.g. a device characteristic), L_j and H_j are user defined boundary specifications for response j; l_i and h_i are bounds upon x_i (design variable i), $FS(\vec{x})$ is the process sensitivity function containing weighted contributions for each response sensitivity. The weights (w_j) allow the process engineer to investigate inevitable trade-off situations. The overall objective function to be optimized is a weighted combination of the target deviation sum of squares objective function and the previously defined process sensitivity objective function. We developed an optimizer (DEBORA) to solve these types of problems. The responses are modeled by truncated Taylor series based upon the results of a chosen experimental design. We developed the TOD concept [2] which allows to compute higher order models in a huge number of variables restricting the model accuracy to the region of interest and consuming a minimum number of experiments. TOD based models are used to identify and rank a number of solution subspaces in the initial design space and to screen out less significant variables. The ranking is based on the sensitivity function. The subspace with the lowest sensitivity will be further investigated using a CCF design after screening out less significant variables. Using the NORMAN/DEBORA TCAD system, we managed to find an optimal process design for our 0.5 μm process in 3 days. We looked at 10 responses which are listed in figure 1. We applied the RSM technique using a TOD in 15 process variables and performed an optimization to minimize the process sensitivity as well as the process target deviations. The optimal solution is compared with an initial solution in figure 4 for 3 responses (threshold voltage for nmos and pmos, leakage current pmos). The process sensitivity is reflected in the spread of the distribution due to normal distributions on the process variables. The target is reflected in the mean of the response distribution. Note that the overall target deviation as well as the overall process sensitivity is reduced.

In addition, we developed a new transformation technique to improve the model accuracy of models based on CCF designs. Each input variable x_i is transformed to $z_i(x_i, \alpha_i, \beta_i)$ (figure 3) by solving iteratively for α_i and β_i in the characteristic ratio equation. The result (figure 5) shows the residual plot, experimented over a 2-D grid, for the original model and the transformed model of a nmos threshold voltage as a function of well dose and well drive-in temperature. The transformation indicates a square root dependence for the well dose agreeing with the physical model for the doping level dependence of the threshold voltage.

3. Simulator calibration

The goal is to tune model coefficients of the simulator such that the difference between experimental and simulated results is minimized. Using the RSM approach, the difference function $\Phi(\vec{x}_s(a_1, \ldots, a_k), \vec{x}_e)$, which is modeled based on the results of an experimental design in the model coefficients (a_i), is minimized ($\vec{x}_e$ is the experimental characteristic and $\vec{x}_s$ is the simulated one). This is shown for the threshold voltage of the nmos and pmos in figure 6 (dashed line is before calibration, solid line after calibration and triangles are measurements) where the difference function to be minimized is expressed as :

$$\Phi(\vec{x}_s(a_1, a_2, a_3), \vec{x}_e) = \sum_{i=n,p} (Vt_i(\vec{x}_s(a_1, a_2, a_3)) - Vt_i(\vec{x}_e))^2$$

$\vec{x_s}(a_1, a_2, a_3)$ is the simulated $I_{ds} - V_{gs}$ characteristic with a_1 being the boron segregation coefficient, a_2 being a pre-exponential coefficient of positive vacancy states (boron diffusion) and a_3 being a coefficient for modelling neutral vacancy states (phosphorus diffusion).

References

[1] R.H. Myers, A.I. Khuri, W.H. Carter, jr. *Response Surface Methodology : 1966-1988*, Technometrics Vol.31, no.2,pp 137-157,1989.

[2] R. Cartuyvels, R. Booth, L. Dupas, K. De Meyer. *Process Technology Optimization Using An Integrated Process and Device Simulation Sequencing System*, ESSDERC '92, Leuven.

response	lower bound	upper bound	target	unit
threshold voltage nmos	0.6	0.7	0.65	V
body effect nmos	*	1.0	$\ll$	$\sqrt{V}$
leakage current nmos	*	10^{-10}	$\ll$	A
max. current nmos	0.001	*	$\gg$	A
max. chan. doping dens. nmos	*	5.E17	$\ll$	cm^{-3}
threshold voltage pmos	-0.7	-0.6	-0.65	V
body effect pmos (abs. value)	*	0.8	$\ll$	$\sqrt{V}$
leakage current pmos (abs. value)	*	10^{-10}	$\ll$	A
max. current pmos (abs. value)	0.001	*	$\gg$	A
max. chan. doping dens. pmos	*	5.E17	$\ll$	cm^{-3}

Figure 1: response specifications ; '*' means 'no bound' ; '$\ll$' means 'as low as possible' ; '$\gg$' means 'as high as possible'

$$\min FS(x_1,\ldots,x_n)$$

subject to

$$\begin{array}{ccccccc} L_j & \le & R_j(\vec{x}) & \le & H_j & \text{j=1..m} \\ l_i & \le & x_i & \le & h_i & \text{i=1..n} \end{array}$$

where

$$\begin{aligned} FS(\vec{x}) &= \sum_{j=1}^{m} w_j FS_j(\vec{x}) \\ FS_j(\vec{x}) &= \sum_{i=1}^{n} \left(\frac{\partial R_j(\vec{x})}{\partial x_i}\right)^2 \\ \vec{x} &= (x_1,\ldots,x_n) \end{aligned}$$

Figure 2: process sensitivity optimization

original model

$$F(\vec{x}) = a_0 + a_1x_1 + \ldots + a_nx_n + a_{1.2}x_1x_2 + \ldots + a_{n-1.n}x_{n-1}x_n + a_{1.1}x_1^2 + \ldots + a_{n.n}x_n^2$$

transformed model

$$T(\vec{z}) = b_0 + b_1z_1 + \ldots + b_nz_n + b_{1.2}z_1z_2 + \ldots + b_{n-1.n}z_{n-1}z_n$$

with

$$z_i(x_i,\alpha_i,\beta_i) = \frac{[(x_i+\beta^2+1)^{\alpha}-1]}{\alpha}$$

Figure 3: model transformations (Box-Cox)

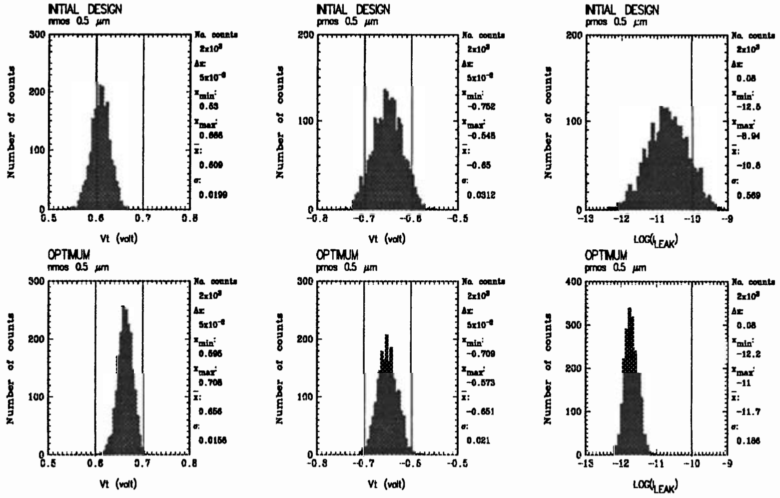

Figure 4: histogram plots of an initial (up) and optimal (down) design

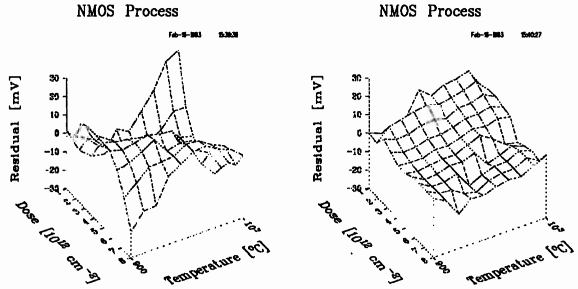

Figure 5: residual for a Vt response (left = original, right = transformed)

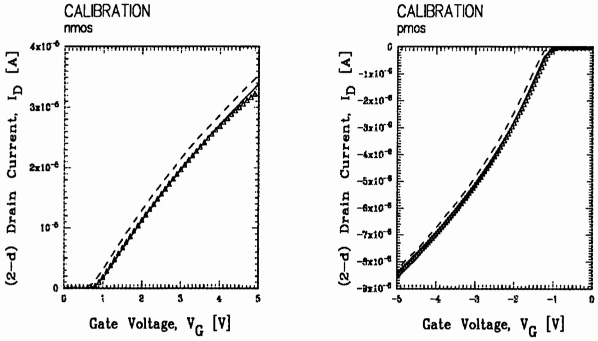

Figure 6: process calibration for accurate threshold voltage prediction